Short-range order in Ising-like models with many-body interactions: Description via effective pair interactions

W. Schweika
Institut für Festkörperforschung der Kernforschungsanlage Jülich, D-5170 Jülich, Federal Republic of Germany

A. E. Carlsson
Department of Physics, Washington University, St. Louis, Missouri 63130
(Received 16 March 1989)

The validity of approximating the effects of many-body interactions in Ising-type models by several types of pair interactions is examined. In addition to the bare pair interaction (P_0), two interactions derived via high-temperature approximations are considered. The first (P_1) is concentration dependent and is obtained by an expansion to first order in inverse temperature; the second (P_2), obtained by a second-order expansion, is both temperature and concentration dependent. The validity of the pair approximations is evaluated by Monte Carlo calculations of ordering and thermodynamic properties for a particular many-body interaction model on a fcc lattice. In the high-temperature limit, the structure (as described by pair and multiple correlation functions) is accurately obtained by both the interactions P_1 and P_2, but not by P_0. Over a much wider range of temperatures, P_2 still yields accurate results. However, none of the pair interaction models obtain accurate mixing enthalpies. The connections that are derived between the strength of the many-body interactions, and the environmental dependence of the effective pair interactions, provide a possible way of evaluating the importance of the many-body interactions in solid solutions from diffuse scattering measurements.

I. INTRODUCTION

Even the simplest alloy systems that can be studied experimentally contain significant three-body and higher-order interactions, and hence cannot be accurately treated by simple Ising-type pair models.[1] This is clear from the asymmetry in the observed phase diagrams, and also from the fact that pair interactions derived from one class of properties, such as correlation functions, often give poor results when applied to other properties, such as heats of formation. In addition, non-negligible higher-order interactions are obtained both by scattering-theoretic analyses,[2] in which a subset of the terms in a perturbative expansion yields the pair interaction, and in matching schemes,[3] which fit pair and cluster interactions to quantum mechanically obtained total energies. However, a description in terms of *effective* pair interactions,[1-5] which treat only a limited part of configuration space, is useful for two reasons. First, the intuitive connection between the interaction parameters and physical properties, such as short-range order, is much clearer and more direct for the pair terms than for the higher-order terms. Thus they constitute a convenient abbreviated description of the energetics of the alloy. Second, we have no experimental techniques which measure multiatom interactions in the bulk. In contrast, detailed and precise measurements of pair-correlation functions in disordered alloys (which describe the short-range order), have been performed during the past two decades. Since 1968, the Krivoglaz-Clapp-Moss (KCM) formula,[6,7] a mean-field approximation, has been used widely to analyze the experimental results in terms of effective pair interactions. The recently developed inverse Monte Carlo method,[8,9] which is more sophisticated than the KCM formula, allows us to determine a unique effective pair interaction from the measured short-range order parameters, on the basis of the principle of detailed balance. It is important to establish whether or not the pair short-range order yields sufficient information to determine the magnitudes of many-body interactions as well, which can be important in the systems that have been studied. More generally, the questions considered here are relevant not only for alloys but for all equivalent systems belonging to the same universality class.

The main purposes of this paper are to evaluate the legitimacy of pair descriptions of short-range order, to obtain explicit relations between the effective pair interactions and the many-body interactions, and to establish the manner in which the pair interactions depend on the properties of the environment, in particular concentration and temperature. To accomplish these tasks, we perform Monte Carlo calculations of the short-range order above the transition temperature T_t for several pair interaction models and one multiatom interaction model on a fcc lattice. Finding existing types of effective pair interactions inadequate for our purposes, we generate a new type of pair interaction which, in addition to the usual dependence on concentration, contains a term proportional to the inverse temperature. This term is obtained from the terms in a high-temperature expansion of the short-range order which are quadratic in the inverse

 ©1989 The American Physical Society

temperature and either linear or quadratic in the multiatom interaction parameters. The inclusion of this simple temperature dependence improves the short-range order results dramatically. For example, at $T=1.5T_t$, the error in the second-neighbor short-range order parameter is reduced to below 5%, from the 20% error obtained by temperature-independent pair interactions. Since the temperature and concentration dependence of the pair interaction are related in a simple fashion to the higher-order interaction parameters, our results show great promise for the possibility of extracting information about cluster interactions from measured short-range order data. The success of the pair interactions in describing short-range order tempts one to apply them to other properties as well. However, our calculated results for the heat of formation show that the temperature-dependent interactions are by no means a universal panacea; in fact, both of the environmentally dependent interactions that we have used give worse results for this quantity than the bare, concentration-independent, pair interaction.

The organization of the remainder of the paper is as follows. Section II describes our cluster interaction model and the analysis underlying the various effective pair interactions which we use to simulate the effects of the cluster interactions. Section III discusses the Monte Carlo technique we use to treat the statistical mechanics. Section IV presents the comparison of the Monte Carlo results for the cluster interactions with those for the effective pair interactions. Section V summarizes our conclusions.

II. INTERACTION MODELS

A more general model for a binary alloy than the often used pair Ising model can be obtained[10] by including many-body interaction terms:

$$H=V^{(0)}+\sum_i V^{(1)}\sigma_i+\frac{1}{2!}\sum_{i,j}V^{(2)}_{ij}\sigma_i\sigma_j+\frac{1}{3!}\sum_{i,j,k}V^{(3)}_{ijk}\sigma_i\sigma_j\sigma_k+\frac{1}{4!}\sum_{i,j,k,l}V^{(4)}_{ijkl}\sigma_i\sigma_j\sigma_k\sigma_l+\cdots . \quad (1)$$

Here H is the Hamiltonian, and the $\{\sigma_i\}$ are classical spinlike variables, which take on the values $\sigma_i=\pm 1$ according to what type of atom occupies a given site. The first term in H is simply a chemical potential term which fixes $\langle\sigma\rangle$. The next three terms correspond to pair, triplet, and quadruplet interactions, respectively. By using the interaction strengths as adjustable parameters, one can obtain a much better global fit to observed phase diagrams than with pair terms alone.[11] In addition, as mentioned before the higher-order terms are expected from a variety of theoretical calculations. Fits to supercell total energy calculations, for example, have shown[12] that values of $|V^{(3)}/V^{(2)}|$ in Al–transition-metal alloys are typically of order 0.1–0.2, although values as large as 0.3–0.4 can occur. A triplet interaction of this magnitude is sufficiently strong to change the sign of the short-range order coefficient at one end of the phase diagram.[12] Scattering-theoretic calculations[2,4] treating only the changes in the one-electron energy resulting from changes in the alloy's state of order have shown that the various terms in Eq. (1) can be associated with an expansion in powers of the scattering matrices of the alloy constituent atoms relative to a complex effective medium. Such calculations have suggested somewhat smaller values for $|V^{(3)}/V^{(2)}|$ for transition-metal–transition-metal alloys.

On the other hand, an accurate description of observed short-range order data, at a given composition and temperature, can often be obtained including only pair interactions. This suggests that the effects of the three-body terms, at least for some properties, can be subsumed in an effective pair interaction which may depend on composition and temperature. To evaluate the validity of this contention, we have calculated several physical properties of the alloy using both the full cluster model and three pair models. In the simplest case, we have simply ignored all but the $V^{(1)}$ and $V^{(2)}$ terms in Eq. (1). In addition, we have considered two pair models which contain the effects of the higher-order terms in an averaged fashion. In these models, we include only the terms up through the $V^{(4)}$ level, because only these are included in the subsequent simulations.

A. Concentration-dependent, temperature-independent interactions

This type of interaction[12] is closely related to those obtained by the scattering-theoretic methods. It is obtained by using as basic variables the atomic concentration fluctuations $\delta\sigma_i=(\sigma_i-\langle\sigma\rangle)$, rather than the σ_i themselves. By simple rearrangement of terms one obtains

$$H=V^{(0),\mathrm{eff}}(\langle\sigma\rangle)+\frac{1}{2!}\sum_{i,j}V^{(2),\mathrm{eff}}_{ij}(\langle\sigma\rangle)\delta\sigma_i\delta\sigma_j+\frac{1}{3!}\sum_{i,j,k}V^{(3),\mathrm{eff}}_{ijk}(\langle\sigma\rangle)\delta\sigma_i\delta\sigma_j\delta\sigma_k+\frac{1}{4!}\sum_{i,j,k,l}V^{(4),\mathrm{eff}}_{ijkl}(\langle\sigma\rangle)\delta\sigma_i\delta\sigma_j\delta\sigma_k\delta\sigma_l , \quad (2)$$

where

$$V^{(0),\mathrm{eff}}(\langle\sigma\rangle)=N\langle\sigma\rangle V_1+\frac{\langle\sigma\rangle^2}{2!}\sum_{i,j}V^{(2)}_{ij}+\frac{\langle\sigma\rangle^3}{3!}\sum_{i,j,k}V^{(3)}_{ijk}+\frac{\langle\sigma\rangle^4}{4!}\sum_{i,j,k,l}V^{(4)}_{ijkl} ,$$

$$V^{(2),\mathrm{eff}}_{ij}(\langle\sigma\rangle)=V^{(2)}_{ij}+\langle\sigma\rangle\sum_k V^{(3)}_{ijk}+\frac{\langle\sigma\rangle^2}{2!}\sum_{k,l}V^{(4)}_{ijkl} ,$$

$$V^{(3),\mathrm{eff}}_{ijk}(\langle\sigma\rangle)=V^{(3)}_{ijk}+\langle\sigma\rangle\sum_l V^{(4)}_{ijkl} ,$$

and

$$V_{ijkl}^{(4),\text{eff}}(\langle\sigma\rangle)=V_{ijkl}^{(4)} . \tag{3}$$

The $V^{(0),\text{eff}}$ term is simply the energy of a completely random alloy having the concentration corresponding to $\langle\sigma\rangle$. The $V^{(1),\text{eff}}$ term is absent because $\sum_i \delta\sigma_i=0$. Note that if $V^{(2)}$, $V^{(3)}$, and $V^{(4)}$ contain only nearest-neighbor terms on a fcc lattice, then the interactions $V^{(i),\text{eff}}$ also contain only nearest-neighbor contributions. $V^{(4),\text{eff}}$ is concentration independent only because we ignore the five-body and higher-order interactions. We include the expressions for $V^{(3),\text{eff}}$ and $V^{(4),\text{eff}}$ here primarily because they will be essential in the subsequent calculation of temperature-dependent potentials.

The main utility of the effective pair interaction is that it is guaranteed to produce the correct short-range order (SRO) at high temperatures. The exact SRO parameters are given by

$$\langle\delta\sigma_i\delta\sigma_j\rangle=Z^{-1}\sum_{\{C\}}\delta\sigma_i\delta\sigma_j e^{-H(\{C\})/k_BT} , \tag{4}$$

where

$$Z=\sum_{\{C\}} e^{-H(\{C\})/k_BT} ,$$

and $\{C\}$ denotes the collection of possible configurations of the alloy. By expansion of the right-hand side of (4) to order $(1/k_BT)$, using the expression (2) for H, one readily obtains (for $i\neq j$) the first-order high-temperature approximation

$$\begin{aligned}\langle\delta\sigma_i\delta\sigma_j\rangle &\approx\langle\delta\sigma_i\delta\sigma_j\rangle^{(1)}\\ &=-(1-\langle\sigma\rangle^2)^2V^{(2),\text{eff}}(i,j;\langle\sigma\rangle)/k_BT .\end{aligned} \tag{5}$$

Thus $V^{(3),\text{eff}}$ and $V^{(4),\text{eff}}$ do not contribute to the SRO to this order in $(1/k_BT)$. It is not clear, however, to what extent such interactions can describe SRO at temperatures comparable to the order-disorder temperature. The subsequent analysis, and the results to be presented in Sec. IV, will provide a partial answer to this question.

B. Concentration and temperature-dependent pair interactions

We expect that a more accurate description of SRO can be obtained if one forces the pair interaction to obtain the correct SRO not just to first order, but also to second order, in $(1/k_BT)$. To evaluate the utility of this approach, we have determined such pair interactions for the model described in Sec. II. The first step in this procedure is the evaluation of the short-range order parameters by expansion of Eq. (4) to second order in $(1/k_BT)$, using the expression (2) for H. The procedure is straightforward but somewhat tedious. The result for interactions of arbitrary range, is the following:

$$\langle\delta\sigma_i\delta\sigma_j\rangle\approx\langle\delta\sigma_i\delta\sigma_j\rangle^{(1)}+\langle\delta\sigma_i\delta\sigma_j\rangle^{(2)} , \tag{6}$$

Here $\langle\delta\sigma_i\delta\sigma_j\rangle^{(1)}$ is given by Eq. (5), and

$$\langle\delta\sigma_i\delta\sigma_j\rangle^{(2)}=(A+B+C+D+E+F)/(k_BT)^2 , \tag{7}$$

where the six contributions to the right-hand side come from six possible types of pairings of pair, triplet, and quadruplet terms. Explicitly,

$$A=\delta_2^3\sum_k V_{ik}^{(2),\text{eff}}(\langle\sigma\rangle)V_{jk}^{(2),\text{eff}}(\langle\sigma\rangle)+\tfrac{1}{2}\delta_3^2V_{ij}^{(2),\text{eff}}(\langle\sigma\rangle)^2 , \tag{8a}$$

$$B=2\delta_3\delta_2^3\sum_k V_{ik}^{(2),\text{eff}}(\langle\sigma\rangle)V_{ijk}^{(3),\text{eff}}(\langle\sigma\rangle) , \tag{8b}$$

$$C=\tfrac{1}{2}\delta_2^2\sum_{k,l} V_{kl}^{(2),\text{eff}}(\langle\sigma\rangle)V_{ijkl}^{(4),\text{eff}}(\langle\sigma\rangle) , \tag{8c}$$

$$D=\tfrac{1}{2}\delta_2^4\sum_{k,l} V_{ikl}^{(3),\text{eff}}(\langle\sigma\rangle)V_{jkl}^{(3),\text{eff}}(\langle\sigma\rangle)+\tfrac{1}{2}\delta_3^2\delta_2\sum_k V_{ijk}^{(3),\text{eff}}(\langle\sigma\rangle)^2 , \tag{8d}$$

$$E=\delta_3\delta_2^3\sum_{k,l} V_{ikl}^{(3),\text{eff}}(\langle\sigma\rangle)V_{ijkl}^{(4),\text{eff}}(\langle\sigma\rangle) , \tag{8e}$$

and

$$F=\tfrac{1}{6}\delta_2^5\sum_{k,l,m} V_{iklm}^{(4),\text{eff}}(\langle\sigma\rangle)V_{jklm}^{(4),\text{eff}}+\tfrac{1}{4}\delta_3^2\delta_2^2\sum_{k,l} V_{ijkl}^{(4),\text{eff}}(\langle\sigma\rangle)^2 , \tag{8f}$$

where

$$\delta_2=\langle(\delta\sigma_i)^2\rangle=1-\langle\sigma\rangle^2 ,$$

and

$$\delta_3=\langle(\delta\sigma_i)^3\rangle=-2\langle\sigma\rangle\delta_2 .$$

If only nearest-neighbor terms are included on a fcc lattice, as in the calculations to be described in Sec. IV, there is only one pair interaction $V^{(2),\text{eff}}$, one triplet interaction $V^{(3),\text{eff}}$, and one quadruplet interaction $V^{(4),\text{eff}}$. The expressions (8) then simplify considerably. We obtain, for nearest-neighbor pairs i and j,

$$\begin{aligned}A&=(4\delta_2^3+\tfrac{1}{2}\delta_3^2)V^{(2),\text{eff}}(\langle\sigma\rangle)^2 ,\\ B&=8\delta_3\delta_2^2V^{(2),\text{eff}}(\langle\sigma\rangle)V^{(3),\text{eff}}(\langle\sigma\rangle) ,\\ C&=2\delta_2^4V^{(2),\text{eff}}(\langle\sigma\rangle)V^{(4),\text{eff}}(\langle\sigma\rangle) ,\\ D&=2(\delta_2^4+\delta_3^2\delta_2)V^{(3),\text{eff}}(\langle\sigma\rangle)^2 ,\\ E&=4\delta_3\delta_2^3V^{(3),\text{eff}}(\langle\sigma\rangle)V^{(4),\text{eff}}(\langle\sigma\rangle) ,\\ F&=\delta_3^2\delta_2^2V^{(4),\text{eff}}(\langle\sigma\rangle)^2 ,\end{aligned} \tag{9a}$$

for second-neighbor pairs i and j,

$$\begin{aligned}A&=4\delta_2^3V^{(2),\text{eff}}(\langle\sigma\rangle)^2 ,\\ D&=4\delta_2^4V^{(3),\text{eff}}(\langle\sigma\rangle)^2 ,\\ B&=C=E=F=0 ,\end{aligned} \tag{9b}$$

for third-neighbor pairs i and j,

$$\begin{aligned}A&=2\delta_2^3V^{(2),\text{eff}}(\langle\sigma\rangle)^2 ,\\ D&=\delta_2^4V^{(3),\text{eff}}(\langle\sigma\rangle)^2 ,\\ B&=C=E=F=0 ,\end{aligned}$$

and for fourth-neighbor pairs i and j

$$A=\delta_2^3 V^{(2),\mathrm{eff}}(\langle\sigma\rangle)^2 ,$$

$$B=C=D=E=F=0 .$$

To obtain the effective temperature-dependent pair interaction, $U^{(2),\mathrm{eff}}(\langle\sigma\rangle,T)$, we evaluate the short-range order parameters to second order in $U^{(2),\mathrm{eff}}$, making the replacement

$$H\rightarrow H^{\mathrm{eff}}(T)=U^{(0),\mathrm{eff}}(\langle\sigma\rangle,T)+\tfrac{1}{2}\sum_{i,j}U_{ij}^{(2),\mathrm{eff}}(\langle\sigma\rangle,T)\delta\sigma_i\delta\sigma_j . \quad (10)$$

Here $U^{(0),\mathrm{eff}}(\langle\sigma\rangle,T)$ is simply a concentration-dependent enthalpy term which does not affect the short-range order. From (5)–(8), we obtain

$$\langle\delta\sigma_i\delta\sigma_j\rangle=-\delta_2^2U_{ij}^{(2),\mathrm{eff}}(\langle\sigma\rangle,T)/k_BT+\delta_2^3\sum_k U_{ik}^{(2),\mathrm{eff}}(\langle\sigma\rangle,T)U_{jk}^{(2),\mathrm{eff}}(\langle\sigma\rangle,T)/(k_BT)^2+\tfrac{1}{2}\delta_3^2U_{ij}^{(2),\mathrm{eff}}(\langle\sigma\rangle,T)^2/(k_BT)^2+O((k_BT)^{-3}) . \quad (11)$$

We demand that (11) and (6) should agree to order $(1/k_BT)^2$. To order $(1/k_BT)$, only the first term on the right-hand side of (11) contributes. Comparing (11) with (5), we then have

$$U_{ij}^{(2),\mathrm{eff}}(\langle\sigma\rangle,T=\infty)=V_{ij}^{(2),\mathrm{eff}}(\langle\sigma\rangle) .$$

Assuming $U^{(2),\mathrm{eff}}$ to vary smoothly with $(1/k_BT)$, we obtain

$$U_{ij}^{(2),\mathrm{eff}}(\langle\sigma\rangle,T)=V_{ij}^{(2),\mathrm{eff}}(\langle\sigma\rangle)+O(1/k_BT) .$$

To order $(1/k_BT)^2$, the right-hand side of (11) is unchanged if $U^{(2),\mathrm{eff}}$ is replaced by $V^{(2),\mathrm{eff}}$ in all terms except the first. Then, comparing (11) with (6) and (7), we have that

$$U_{ij}^{(2),\mathrm{eff}}(\langle\sigma\rangle,T)=V_{ij}^{(2),\mathrm{eff}}(\langle\sigma\rangle)-(B+C+D+E+F)/(\delta_2^2k_BT) .$$

With only nearest-neighbor interactions on a fcc lattice in the starting Hamiltonian, we obtain via Eq. (9) for a nearest-neighbor pair i and j,

$$U_{ij}^{(2),\mathrm{eff}}(\langle\sigma\rangle,T)=V^{(2),\mathrm{eff}}(\langle\sigma\rangle)-[8\delta_3V^{(2),\mathrm{eff}}(\langle\sigma\rangle)V^{(3),\mathrm{eff}}(\langle\sigma\rangle)+2\delta_2^2V^{(2),\mathrm{eff}}(\langle\sigma\rangle)V^{(4),\mathrm{eff}}(\langle\sigma\rangle)+2(\delta_2^2+\delta_3^2/\delta_2)V^{(3),\mathrm{eff}}(\langle\sigma\rangle)^2+4\delta_3\delta_2V^{(3),\mathrm{eff}}(\langle\sigma\rangle)V^{(4),\mathrm{eff}}(\langle\sigma\rangle)+\delta_3^2V^{(4),\mathrm{eff}}(\langle\sigma\rangle)^2]/k_BT , \quad (12a)$$

for second- and third-neighbor pairs,

$$U_{ij}^{(2),\mathrm{eff}}(\langle\sigma\rangle,T)=-4\delta_2^2V^{(3),\mathrm{eff}}(\langle\sigma\rangle)^2/k_BT , \quad (12b)$$

and

$$U_{ij}^{(2),\mathrm{eff}}(\langle\sigma\rangle,T)=-\delta_2^2V^{(3),\mathrm{eff}}(\langle\sigma\rangle)^2/k_BT , \quad (12c)$$

respectively; all farther interactions vanish.

We now turn to the physical interpretation of these effective potentials. We treat first the $\delta_2^2(V^{(3),\mathrm{eff}})^2$ terms, which contribute at the first-, second-, and third-neighbor separations. These contributions to $U^{(2),\mathrm{eff}}$ are manifestly negative, favoring ferromagnetic ordering. They arise from the terms in the short-range order expansion given by the first half of the right-hand side of Eq. (8d). These terms arise from pairs of nearest-neighbor triangles such that site i is at a vertex of one triangle, site j is at a vertex of the second triangle, and the sites k and l are shared by both triangles. If we take, for example, $\sigma_i=+1$ and $V^{(3),\mathrm{eff}}(\langle\sigma\rangle)>0$, the three-body terms in the energy will first result in an antiferromagnetic (negative) contribution to $\delta\sigma_k\delta\sigma_l$; subsequently the three-body terms involving the interaction of this pair with σ_j will favor $\sigma_j=+1$ over $\sigma_j=-1$. Thus the short-range order parameters behave as if there were an extra ferromagnetic term coupling the sites i and j. An entirely parallel argument holds for the case $V^{(3),\mathrm{eff}}(\langle\sigma\rangle)<0$. The relative magnitudes of the first-, second-, and third-neighbor terms result simply from the numbers of pairs of nearest-neighbor triangles of the above type; for nearest neighbors there are two such pairs, for second neighbors there are four, but for third neighbors there is only one. The prefactors of these terms vanish when $\langle\sigma\rangle^2=1$. This reflects the fact that the magnitude of the contribution to $\delta\sigma_k\delta\sigma_l$ resulting from a particular atom at site i must vanish when the minority concentration vanishes. One might expect similar contributions from $(V^{(4),\mathrm{eff}})^2$ terms; these vanish in the fcc structure because there are no pairs of nearest-neighbor tetrahedra sharing a common face.

The remaining contributions are present only in the nearest-neighbor interaction. The $\delta_3V^{(2),\mathrm{eff}}V^{(3),\mathrm{eff}}$ term is due to the term (B) [cf. Eq. (8)] in $\langle\delta\sigma_i\delta\sigma_j\rangle^{(2)}$, which consists of contributions from nearest-neighbor triangles containing the sites i and j. The origin of this term may be understood as follows. Assume that $V^{(2),\mathrm{eff}}$ and $V^{(3),\mathrm{eff}}$ are positive, and that $\sigma_i=+1$. Then the $V^{(2),\mathrm{eff}}$ terms in H will make a negative contribution to $\langle\delta\sigma_k\rangle$. The

$V^{(3),\text{eff}}$ terms, in turn, will result in a positive contribution to $\langle \delta\sigma_j \rangle$, so that the net contribution to $\langle \delta\sigma_i \delta\sigma_j \rangle$ is ferromagnetic. On the other hand, if $\sigma_i = -1$, the net contribution to $\langle \delta\sigma_i \delta\sigma_j \rangle$ is antiferromagnetic. The relative probabilities of these two cases are determined by $\langle \sigma \rangle$, and are such that the total contribution to $\langle \delta\sigma_i \delta\sigma_j \rangle$ is ferromagnetic if $\langle \sigma \rangle > 0$. The $\delta_3 V^{(3),\text{eff}} V^{(4),\text{eff}}$ terms in (12a) may be understood by a completely parallel analysis of the term E in Eq. (8).

Finally, the $\delta_3^2/\delta_2 (V^{(3),\text{eff}})^2$ terms in (12a) arise from the corresponding terms in (8d) which came from nearest-neighbor triangles containing the sites i and j. These terms, in turn, arise from contributions to the probability distribution proportional to $\delta\sigma_i^2 \delta\sigma_j^2 \delta\sigma_k^2$. If $\langle \sigma \rangle > 0$ these terms are largest for $\sigma_i = \sigma_j = \sigma_k = -1$, if $\langle \sigma \rangle < 0$ they are maximized for $\sigma_i = \sigma_j = \sigma_k = 1$, and if $\langle \sigma \rangle = 0$, they are independent of configuration. Thus for $\langle \sigma \rangle \neq 0$ they produce a net ferromagnetic contribution to the short-range order.

III. MONTE CARLO TECHNIQUE

In the previous section we have obtained effective pair interactions which approximate the many-body interactions in increasing orders of $(1/k_B T)$. To investigate the validity of these high-temperature approximations we have performed Monte Carlo simulations in the solid solution region of the disordered phases. In order to compare the configurations obtained by the various interaction schemes, we have determined the pair correlation function, cluster probabilities, and configurational energies as functions of the temperature and the concentration.

According to the purpose of the present investigation, our Monte Carlo simulations are focused primarily on the pair correlations in the disordered phase, and further on those cases where one expects the largest differences between the cluster interaction model and the approximations by effective pair interactions. Therefore, most of the simulations were performed at the A_3B stoichiometry for the model considered. As will become apparent from our results on the correlation functions, we need high precision in the Monte Carlo simulation to distinguish between the results of the various interaction schemes.

The many-body interaction model we have studied here is chosen because it has been already treated[11] in the literature as a model for the Cu-Au alloy. The order-disorder phase diagram has been calculated by both the cluster variation method[11] and the Monte Carlo method.[13] There has been a long standing controversy about whether the triple points are at zero temperature, as given in the published Monte Carlo results,[13] or at finite temperatures, as was found first by the cluster variation method.[11] In our Monte Carlo simulations we find clear evidence that the triple points are at finite temperatures for nearest-neighbor interaction models for pair interaction models as well as for cluster interaction models. Except on this point, our results agree with the previously calculated phase diagram of Styer *et al.* We emphasize that we do not expect this model to describe the real interactions and correlations in CuAu alloys. However, the calculated phase diagram shows a reasonable likeness to the observed CuAu phase diagram.

We performed the simulations[14] on a fcc lattice of 108 000 sites. We used both the single-spin-flip kinetics (Glauber dynamics) and the nearest-neighbor exchange kinetics (Kawasaki). In general, the relaxation to the equilibrium will be faster for the calculation in the grand canonical ensemble (single-spin flip). However, for the present purpose of comparing results at a given temperature and concentration, the canonical ensemble (nearest-neighbor exchange) is more advantageous; triplet and higher-order correlation functions are increasingly sensitive to small deviations in concentration. The computations were performed on a CRAY-XMP at the Kernforschungsanlage Jülich. Since we used a vectorized program, more than a million Monte Carlo steps (MCS's) per CPU second were achieved.

The values for the pair-correlation function were obtained from simulations above the transition temperatures. For the comparison between the models it is important to regard the details in the full range of the correlation function. Therefore, at lower temperatures (i.e., 1.5 times the transition temperature or less), at which the correlation length grows, we calculated the pair-correlation function up to 80 neighboring shells for detailed comparisons. Since the temperatures of the simulations are not very close to the transition temperatures, less than 100 Monte Carlo steps per site were needed to equilibrate the system. Starting from random configurations after 300 MCS's per site for equilibration, the averages were taken from 50 configurations during the following 1000 MCS's per site. Because of the large size of the system, 108 000 atoms, accurate values for the pair-correlation function were obtained, with an error of roughly 0.001.

At lower temperatures the comparisons are also affected more by the precise location of the ordering spinodal (or the transition temperature for *second*-order transitions). The transitions from the ordered $L1_2$ phase of the A_3B alloy to the disordered fcc phase are of first order. Starting from initially ordered configurations, the transition temperatures were determined from the discontinuities in the internal energy and the order parameter. However, this work is more focused on the configurations in the disordered phase, because such configurations can be measured very accurately by diffuse (neutron) scattering and effective pair interactions can be determined from such experimental data using the inverse Monte Carlo method.[8,9]

IV. RESULTS

To assess the utility of the pair interactions described above, for physically reasonable parameters, we have used values of the cluster interactions which have previously been applied[11] to the Cu-Au phase diagram: For nearest-neighbor clusters, $V^{(2)} = 30$ meV, $V^{(3)} = -1.025$ meV, and $V^{(4)} = -1.575$ meV. (In the notation of Ref. 11, these correspond to $V_0 = 60$ meV, $\alpha = -0.08$, and $\beta = 0.01$.) All other interactions are neglected. The sign of $V^{(3)}$ is such that an Au(Cu) site has $\sigma = +1(-1)$.

These parameters cannot quantitatively describe the energetics of Cu-Au alloys, for several reasons, including the presence of significant second-neighbor interactions.[15] However, they do reproduce the observed order-disorder temperatures, and correspond to physically reasonable higher-order interactions. The cluster interactions are quite weak compared to typical Al-transition metal systems, for which[12] (as mentioned previously)

$$|V^{(3)}/V^{(2)}| \sim 0.1-0.2 \ .$$

For our systematic analysis, we focus on the $Cu_{0.25}Au_{0.75}$ stoichiometry. A smaller set of calculations at other stoichiometries has resulted in similar conclusions.

The first approximation to the cluster interaction model, going beyond the bare pair interaction $V^{(2)}$, is given by the concentration dependent effective pair interaction $V^{(2),\text{eff}}$, which is shown in Fig. 1(a). The drop in $V^{(2),\text{eff}}$ with increasing $\langle \sigma \rangle$ is readily understood via Eq. (3) and the negative sign of $V^{(3)}$. Figure 1(b) displays the calculated temperature-dependent interactions $U_{ij}^{(2),\text{eff}}$ for a $Cu_{0.25}Au_{0.75}$ ($\langle \sigma \rangle = 0.5$) alloy, down to temperatures slightly below the order-disorder transition temperature T_t obtained by the full cluster Hamiltonian. At $T=\infty$, $U^{(2),\text{eff}} = V^{(2),\text{eff}}$, and the corrections to $V^{(2)}$ resulting from $V^{(3)}$ and $V^{(4)}$ amount to a 10% reduction in magnitude at the nearest-neighbor distance. The second- and third-neighbor corrections vanish at $T=\infty$, since, as discussed above, $V^{(2),\text{eff}}$ contains only nearest-neighbor couplings. With dropping temperature the nearest-neighbor coupling receives a significant ferromagnetic contribution which reduces its magnitude by an additional 20% at T_t. This contribution is dominated by the $V^{(2),\text{eff}}V^{(3),\text{eff}}$ and $V^{(2),\text{eff}}V^{(4),\text{eff}}$ terms [cf. Eq. (12)], as expected from the small values of the cluster interactions relative to the pair terms ($V^{(2),\text{eff}}=27.2$ meV, $V^{(3),\text{eff}}=-1.8$ meV, $V^{(4),\text{eff}}=-1.6$ meV). The second- and third-neighbor terms are entirely due to the $(V^{(3),\text{eff}})^2$ contributions and are smaller than the nearest-neighbor corrections, by more than a factor of 50.

In Fig. 2 we display the temperature dependence of the first- and second-neighbor short-range order parameters α_1 and α_2. These parameters are defined by

$$\alpha_n = \langle \delta\sigma_0 \delta\sigma_i \rangle / (1-\langle \sigma \rangle^2) \ ,$$

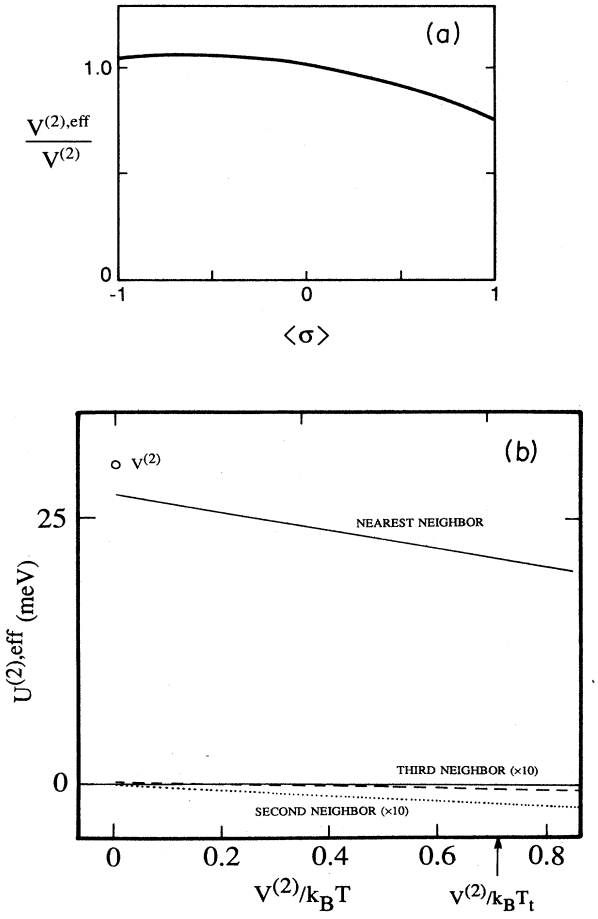

FIG. 1. (a) Concentration-dependent pair interaction, normalized to $V^{(2)}=30$ meV. (b) Concentration- and temperature-independent interaction vs inverse temperature. T_t denotes transition temperature.

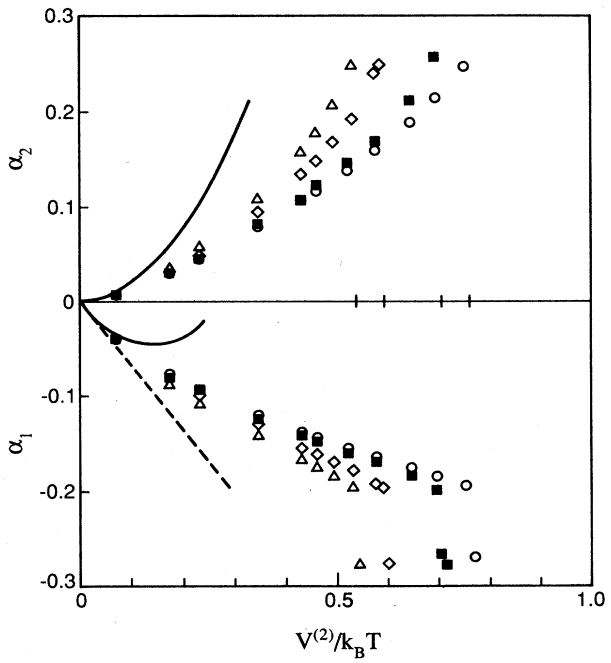

FIG. 2. Short-range order parameters, at first (α_1) and second (α_2) neighbor distances: $V^{(2)}=30$ meV. Solid squares: full cluster Hamiltonian [Eq. (1)]. Triangles: bare pair interaction only. Diamonds: concentration-dependent interaction $V^{(2),\text{eff}}$ [Eq. (3)]. Circles: concentration- and temperature-dependent interaction $U^{(2),\text{eff}}$ [Eq. (12)]. Dashed and solid lines denote first- and second-order expansions in inverse temperature, respectively. Transition temperatures for the various models indicated by marks on the horizontal axis.

where i is any site in the nth neighbor shell of site 0. We show results for four different models: (1) the full cluster Hamiltonian [Eq. (1)], (2) only the pair terms $V^{(2)}$ in this Hamiltonian, (3) the temperature-independent effective pair interaction $V^{(2),\text{eff}}$ [Eq. (3)], and (4) the temperature-dependent effective pair interactions $U^{(2),\text{eff}}$ [Eq. (12)]. In addition, high-temperature expansions to first and second order in $(1/k_BT)$ [cf. Eqs. (6)–(8)] are shown. [For α_2 the $(1/k_BT)$ contribution vanishes and is not shown.] We see that the first-order high-temperature expansion for α_1 results in errors of 10% already at $T\approx 10V^{(2)}/k_B$ ($\approx 10T_t$); the second-order expansion improves on this result somewhat but causes gross discrepancies at $T\approx 5V^{(2)}/k_B$ and below. On the other hand, the temperature-dependent potential $U^{(2),\text{eff}}$ produces excellent results even quite close to T_t. The results for α_2 are roughly similar, with the second-order expansion producing errors of roughly 30% at $T=5V^{(2)}/k_B$ and much larger errors at lower temperatures. The $U^{(2),\text{eff}}$ results are very close to the Monte Carlo results and improve considerably on both the $V^{(2)}$ and $V^{(2),\text{eff}}$ results. The error of the latter is roughly half of that for $V^{(2)}$, but is still an order of magnitude greater than that for $U^{(2),\text{eff}}$ at temperatures comparable to T_t.

Thus the linear $(1/k_BT)$ dependence of $U^{(2),\text{eff}}$ appears to account for the short-range order much better than the second-order expansion of α_1 and α_2, which was originally used to generate $U^{(2),\text{eff}}$. This cannot be explained by the smallness of the temperature-dependent corrections to the pair interactions or the higher-order interactions, since these effects are indicated by the differences between the exact results in Fig. 2 and the $V^{(2),\text{eff}}$ and $V^{(2)}$ curves, respectively. In fact, the exact temperature-dependent pair interaction $U^{(2),\text{ex}}$, which is defined as the interaction which rigorously reproduces the exact short-range order, can be written as

$$U^{(2),\text{ex}}=V^{(2),\text{eff}}+a_3\frac{V^{(3),\text{eff}}V^{(2),\text{eff}}}{k_BT}[1+b_1(V^{(2),\text{eff}}/k_BT)+\cdots]$$
$$+\frac{a_4V^{(4),\text{eff}}V^{(2),\text{eff}}}{k_BT}[1+c_1(V^{(2),\text{eff}}/k_BT)+\cdots]+O((V^{(3),\text{eff}})^2,(V^{(4),\text{eff}})^2,(V^{(3),\text{eff}}V^{(4),\text{eff}}))\ . \tag{13}$$

Thus the terms in $U^{(2),\text{eff}}$ that are linear in $V^{(3),\text{eff}}$ and $V^{(4),\text{eff}}$ correspond to expansions in $V^{(2),\text{eff}}/k_BT$, which are not *a priori* expected to be rapidly convergent near T_t. The reason for the rapid convergence that we have observed may be analogous to the improved convergence obtained by the use of self-energies in perturbative treatments of interacting quantum many-particle systems. The self-energy converges more rapidly in series expansions because the combinatoric factors associated with various orders in perturbation theory are better behaved for the self-energy than they are for direct expansions of the physically observable correlation functions. Roughly speaking, since the self-energy is less singular than the correlation functions, when viewed as a function of the interaction strength, it seems to be a more natural target for a series expansion. The effective potential $U^{(2),\text{eff}}$ here is closely analogous to the self-energy: instead of including two-body interactions in an effective single-particle potential, as in the case of the self-energy, one includes three- and four-body interactions in an effective two-body potential. Thus a possible reason for the accuracy of the results obtained by $U^{(2),\text{eff}}$ may be that $U^{(2),\text{ex}}$ behaves more smoothly as a function of temperature than do the various correlation functions of interest.

A more detailed picture of the short-range order is given in Fig. 3, which compares the calculated distance-dependent short-range order parameters α_n for the four different models treated in Fig. 2. At $T=5.75V^{(2)}/k_B$ ($\approx 4T_t$) both $V^{(2),\text{eff}}$ and $U^{(2),\text{eff}}$ describe the short-range order very well, but the bare pair interaction $V^{(2)}$ results in errors of 10–20%. This is as expected from Eq. (5), which shows that $V^{(2),\text{eff}}$ must obtain the correct short-range order in the high-temperature limit. The situation at $T=2.16V^{(2)}$ ($\approx 1.5T_t$) is considerably different. At the second-neighbor distance, use of $V^{(2)}$ results in an estimate of α_2 which is high by nearly 50%. The inclusion of the higher-order terms in $V^{(2),\text{eff}}$ improves the situation somewhat, but the error is still over 20%. However, the additional temperature-dependent terms contained in $U^{(2),\text{eff}}$ result in a dramatic improvement, the 5% remaining error being comparable to the numerical error in the Monte Carlo calculations. Similar improvements are seen at the further neighbor separations as well. The close agreement between the $U^{(2),\text{eff}}$ results and the exact cluster results implies that it is impossible, on the basis of measured short-range order data at a single temperature and composition, to distinguish between pair and cluster models for the interaction Hamiltonian. However, as will be discussed in Sec. V, measurements of short-range order at several different concentrations and temperatures, and comparison with other properties such as the heat of formation, *can* supply information about the relative importance of the cluster terms.

In order to assess the utility of the various pair interactions in treating the long-ranged part of the correlations, we have evaluated (cf. Fig. 4) the static structure factor at an ordering wave vector $\mathbf{q}_c$ for the $CuAu_3$ structure:

$$S(\mathbf{q}_c)=\sum_i\langle\delta\sigma_0\delta\sigma_i\rangle e^{i\mathbf{q}_c\cdot\mathbf{R}_i}/(1-\langle\sigma\rangle^2)\ , \tag{14}$$

where

$$\mathbf{q}_c=(2\pi/a)(1,0,0)\ ,$$

and a is the lattice constant. The results follow the pattern set by the preceding ones. At high temperatures all

of the pair interactions provide a reasonably good description of $S(\mathbf{q}_c)$. At lower temperatures, large discrepancies begin to appear for the $V^{(2)}$ and $V^{(2),\text{eff}}$ results, with the latter being more accurate. For all the temperatures considered, the $U^{(2),\text{eff}}$ results are within the Monte Carlo error bars of the exact results. Thus even for the long-ranged part of the correlations, a good description can be obtained by an effective pair interaction.

A more stringent test of the utility of the pair interactions is the calculation of the order-disorder transition

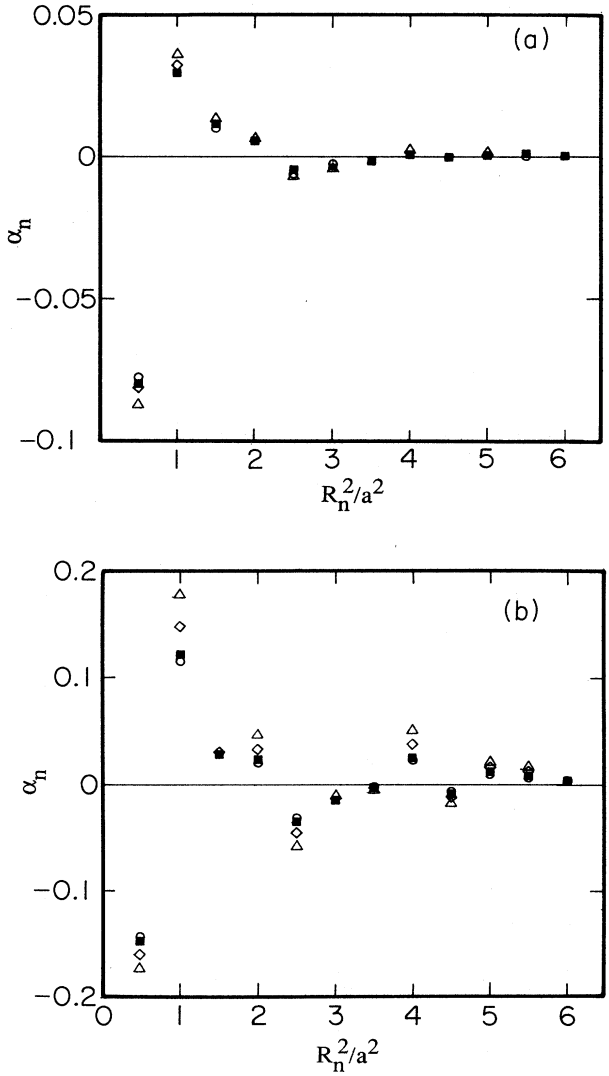

FIG. 3. Short-range order parameters vs interatomic separation R_n; lattice constant for fcc lattice is a. (a) $T=2000$ K$=5.75V^{(2)}/k_B$. (b) $T=750$ K$=2.16V^{(2)}/k_B$. Solid squares: full cluster Hamiltonian [Eq. (1)]. Triangles: bare pair interaction only. Diamonds: concentration-dependent interaction $V^{(2),\text{eff}}$ [Eq. (3)]. Circles: concentration- and temperature-dependent interaction $U^{(2),\text{eff}}$ [Eq. (12)].

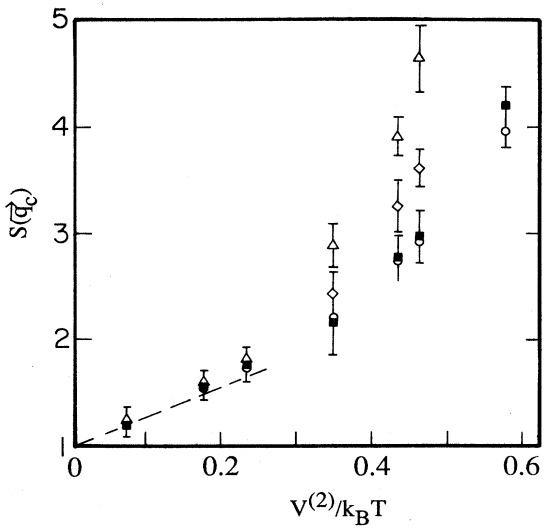

FIG. 4. Structure factor at ordering wave vector for $L1_2$ structure vs inverse temperature: $V^{(2)}=30$ meV. Solid squares: full cluster Hamiltonian [Eq. (1)]. Triangles: bare pair interaction only. Diamonds: concentration-dependent interaction $V^{(2),\text{eff}}$ [Eq. (3)]. Circles: concentration- and temperature-dependent interaction $U^{(2),\text{eff}}$ [Eq. (12)].

temperature, since this involves the free energy of a long-range-ordered state, as well as the short-range-ordered states considered up to now. We have approximately evaluated the transition temperatures T_t for the various models by calculating the temperature dependence of the long-range order parameter. This, in turn, was obtained by starting the system in an artificially ordered state and allowing it to evolve over Monte Carlo steps. *A priori*, we do not expect $U^{(2),\text{eff}}$ to describe the ordered state well, since it is derived from properties of the high-temperature disordered state. However, our results again reveal $U^{(2),\text{eff}}$ to be considerably more accurate than $V^{(2),\text{eff}}$ or $V^{(2)}$. The value of T_t obtained by the full cluster Hamiltonian is roughly

$$490\pm4\text{ K}=1.41V^{(2)}/k_B$$

(versus 493±2 K from Styer *et al.*[13]). The bare pair interaction yields $T_t\approx1.85V^{(2)}/k_B$, more than 30% too high. The temperature-independent effective pair interaction $V^{(2),\text{eff}}$ eliminates less than half of the discrepancy, giving $T_t\approx1.68V^{(2)}/k_B$. Finally the value of $1.31V^{(2)}/k_B$ obtained by $U^{(2),\text{eff}}$ is within 7% of the correct value.

At temperatures significantly below T_t, however, $U^{(2),\text{eff}}$ does not produce useful results. The calculated long-range order parameter displays a very unphysical behavior at lower temperatures, dropping with decreasing temperature below $T=0.9V^{(2)}/k_B$. In fact, for sufficiently low temperatures, it is clear from Eq. (12) that U_2^{eff} must change sign and become ferromagnetic. Thus in the low-temperature limit, either $V^{(2)}$ or $V^{(2),\text{eff}}$ will provide a more accurate description than $U^{(2),\text{eff}}$. However, it may be possible to improve the temperature

dependence of $U^{(2),\text{eff}}$ by going to higher order in $(1/k_BT)$ or by starting with a low-temperature approximation. For example, at very low temperatures, we expect nearest-neighbor Cu triplets or quadruplets to be rare. If one assumes that they are absent, one can obtain the pair and triplet correlation functions entirely in terms of the pair correlation function. One then obtains a nearest-neighbor effective pair interaction equal to

$$V^{(2)}+4V^{(3)}+2V^{(4)}=V^{(2),\text{eff}}(\langle\sigma\rangle=1)$$
$$=22.8 \text{ meV},$$

which yields the accurate estimate $T_t=1.42V^{(2)}/k_B$ for the transition temperature. We do not at present have a well-justified prescription for interpolating between this low-temperature result and the high-temperature interaction $U^{(2),\text{eff}}$.

Up to this point we have considered only pair correlations, which were also used as inputs for the interaction $U^{(2),\text{eff}}$ (although only at high temperatures). A more complete picture of the structure of the alloy is given by the actual fractional numbers of tetrahedra of various types, which reflect the triplet and quadruplet correlations obtained in the Monte Carlo simulations. The values of the fraction of $CuAu_3$ tetrahedra are displayed in Fig. 5. At infinite temperature all the approximations must give the completely random value $(0.75)^3(0.25)(4)=0.422$; at zero temperature, all tetrahedra are $CuAu_3$ and the fraction is unity. Because $V^{(2)}$ is the strongest of the three pair interactions that were used, the $V^{(2)}$ curve climbs more rapidly than those for $V^{(2),\text{eff}}$ and $U^{(2),\text{eff}}$. Replacement of $V^{(2)}$ by $V^{(2),\text{eff}}$ reduces the discrepancy with the full cluster results by nearly 50%; the inclusion of the temperature dependence in $U^{(2),\text{eff}}$ places the pair interaction results within the error bars of the Monte Carlo results.

The last alloy property which we treat is the heat of formation. Let us assume that we have determined effective pair interactions by the inverse Monte Carlo method. Since we do not *a priori* know the magnitude of the possible contributions from the many-body terms, we would calculate the heats of mixing just from the pair terms in Eqs. (2) and (10). However, this means that possible cluster contributions to the single-site terms in these expressions are neglected. Therefore, heats of formation calculated in this fashion should be different from the measured data if many-body interactions are present in the alloy. This point is illustrated in Fig. 6. We see that $U^{(2),\text{eff}}$ describes the heat of formation poorly. In fact, for the completely random solid solution ($T=\infty$), the bare pair interaction $V^{(2)}$ gives a more accurate heat of formation than either $V^{(2),\text{eff}}$ or $U^{(2),\text{eff}}$. For more ordered solutions, corresponding to lower temperatures, the $V^{(2),\text{eff}}$ results improve somewhat on those obtained by $V^{(2)}$, but the $U^{(2),\text{eff}}$ results became significantly worse. Discrepancies of this type have already been pointed out in Ref. 8, although the authors of that work suspected that the quality of the experimental short-range order data might be poor; as discussed above, the discrepancies may be due to many-body interactions instead. In fact, if the effective pair interactions are strongly concentration-dependent, the heats of formation based only on these interactions are expected to be inaccurate. One can imagine the formation of a solid solution from blocks of A and B elemental metals as a continuous process involving the transfer of B atoms to the A block and A atoms to the B block, until both blocks have the same composition. In

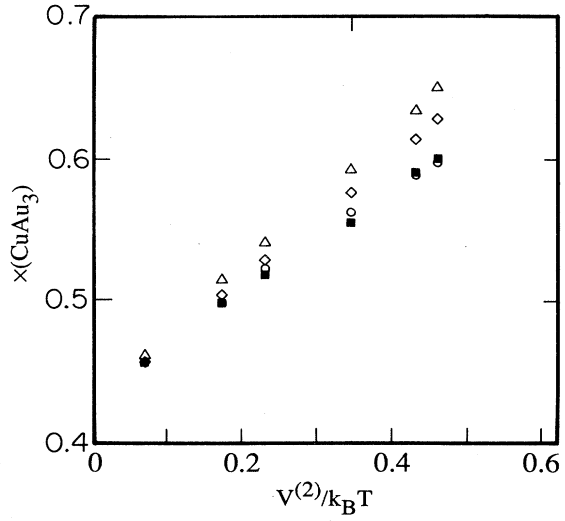

FIG. 5. Fraction of four-atom tetrahedral clusters having $CuAu_3$ stoichiometry, vs inverse temperature: $V^{(2)}=30$ meV. Solid squares: full cluster Hamiltonian [Eq. (1)]. Triangles: bare pair interaction only. Diamonds: concentration-dependent interaction $V^{(2),\text{eff}}$ [Eq. (3)]. Circles: concentration- and temperature-dependent interaction $U^{(2),\text{eff}}$ [Eq. (12)].

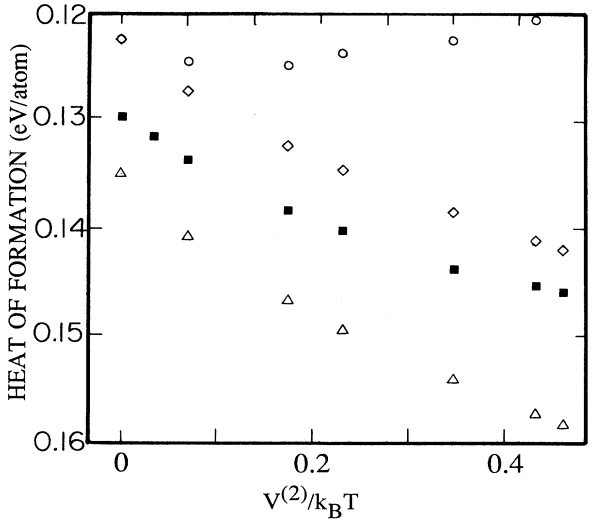

FIG. 6. Heat of formation vs inverse temperature: $V^{(2)}=30$ meV. Solid squares: full cluster Hamiltonian [Eq. (1)]. Triangles: bare pair interaction only. Diamonds: concentration-dependent interaction $V^{(2),\text{eff}}$ [Eq. (3)]. Circles: concentration- and temperature-dependent interaction $U^{(2),\text{eff}}$ [Eq. (12)].

this process, a continuous range of compositions, ranging from pure A to pure B, are sampled. Thus the values of the effective pair interactions at a particular composition are not necessarily relevant, and the pair interactions that describe heats of formation should involve some form of averaging over concentrations. Since the cluster interactions are directly related to the concentration derivatives of the pair interactions [as is seen immediately from Eq. (3)], it may be that to obtain the correct heat of formation one needs to know these derivatives as well as the pair interaction values themselves.

V. CONCLUSIONS

The most surprising feature of the preceding results is the accuracy with which the structure of our model cluster interaction alloy, at temperatures above the transition temperature, can be described by the effective pair interactions. The results for the distribution of tetrahedron types are particularly noteworthy, since this distribution is *directly* influenced by the higher-order interactions, which we average in an approximate fashion; in contrast, the pair short-range order is only indirectly influenced by these interactions. The key to obtaining an accurate, flexible, effective pair interaction lies in including the temperature dependence of the interaction. We have seen that even an approximate treatment of this temperature dependence, including only terms of order $1/k_BT$, can reduce errors in several physical quantities by a factor of 5 or more. The temperature dependence of the pair interaction is much less singular than that of several observable properties of the alloy, which may explain the success of the low-order expansion. However, the structure of the alloy below the transition temperature, and the heat of formation, are described poorly by all of the pair interaction models. For treating these properties, one must either use the complete cluster Hamiltonian, or take into account all of the contributions to the one-body terms.

The preceding results should be of considerable utility in extracting information about higher-order interactions from measured short-range order parameters. From these parameters, one can extract the effective pair interaction $U^{(2),\mathrm{ex}}$ that produces the correct short-range order at a particular temperature. If this interaction produces a poor heat of formation, then one expects that many-body interactions are important. In addition, if one can obtain data at sufficiently high temperatures, the high-temperature approximation $U^{(2),\mathrm{eff}}$ to $U^{(2),\mathrm{ex}}$ will be accurate. Since the temperature dependence of $U^{(2),\mathrm{eff}}$ is explicitly given in terms of the cluster interactions [cf. Eq. (12)], the temperature dependence of the measured interaction can be used to provide direct measurements of certain combinations of the interactions. On the other hand, the concentration dependence of the pair interactions can be related to different combinations of the higher-order terms. Hence, the use of both types of information should allow the determination of the importance, and perhaps the form, of many-body interactions in alloys.

Future work should explore the limits of validity of this technique. We have obtained excellent results for alloy structure using physically reasonable values of the cluster interactions. However, our expansion contains only low-order terms in $V^{(n)}/k_BT$, where $n>2$. Thus we expect the method to break down for sufficiently large cluster interaction values and at low temperatures. In addition it should be established whether or not our approach is accurate for systems with longer-ranged interactions; we have no reason to doubt this, but it needs to be established definitively.

ACKNOWLEDGMENTS

We are grateful for the hospitality of Kernforschungsanlage Jülich during the period under which most of this work was performed. This work was partly supported by the U.S. Department of Energy under Grant No. DE-FG02-84ER45130.

[1]A. Bieber and F. Gautier, Acta Metall. **34**, 2291 (1986); **35**, 1839 (1987).

[2]A. Bieber and F. Gautier, J. Phys. Soc. Jpn. **53**, 2061 (1984).

[3]J. W. D. Connolly and A. R. Williams, Phys. Rev. B **27**, 5168 (1983).

[4]P. E. A. Turchi, G. M. Stocks, W. H. Butler, D. M. Nicholson, and A. Gonis, Phys. Rev. B **37**, 5982 (1988).

[5]A. E. Carlsson, Phys. Rev. Lett. **59**, 1108 (1987).

[6]S. C. Moss and P. C. Clapp, Phys. Rev. **171**, 764 (1968).

[7]M. A. Krivoglaz and A. A. Smirnov, *The Theory of Order-Disorder in Alloys* (MacDonald, London, 1964); M. A. Krivoglaz, *The Theory of X-Ray and Thermal Neutron Scattering by Real Crystals* (Plenum, New York, 1969).

[8]V. Gerold and J. Kern, Acta Metall. **35**, 393 (1987).

[9]W. Schweika and H. G. Haubold, Phys. Rev. B **37**, 9240 (1988).

[10]J. M. Sanchez, F. Ducastelle, and D. Gratias, Physica **128A**, 334 (1984), and references therein; J. M. Sanchez and D. de Fontaine, in *Structure and Bonding in Crystals,* edited by M. O'Keefe and A. Navrotsky (Academic, New York, 1981), Vol. 2, p. 117.

[11]R. Kikuchi and D. de Fontaine, in *Applications of Phase Diagrams in Metallurgy and Ceramics,* National Bureau of Standards (U.S.) Special Publication No. 496 (U.S. Government Printing Office, Washington, D.C., 1978), Vol. 2, p. 967; D. de Fontaine and R. Kikuchi, *ibid.*, p. 999.

[12]A. E. Carlsson, Phys. Rev. B **35**, 4858 (1987); **40**, 912 (1989).

[13]D. F. Styer, M. K. Phani, and J. L. Lebowitz, Phys. Rev. B **34**, 3361 (1986).

[14]For background information on the techniques used here, see *Monte Carlo Methods in Statistical Physics,* edited by K. Binder (Springer, Heidelberg, 1979); *Applications of the Monte Carlo Method in Statistical Physics,* edited by K. Binder (Springer, Heidelberg, 1984).

[15]F. Livet and M. Bessiere, J. Phys. (Paris) **48**, 1703 (1987).